Mid-infrared OCT imaging in highly scattering samples using real-time upconversion of broadband supercontinuum covering from 3.6-4.6 μm

Christian R. Petersen[1,2*], Niels M. Israelsen[1,2], Ajanta Barh[3], Deepak Jain[1], Mikkel Jensen[1], Günther Hannesschläger[4], Peter Tidemand-Lichtenberg[3,5], Christian Pedersen[3,5], Adrian Podoleanu[6] and Ole Bang[1,2,7]

[1] *DTU Fotonik, Technical University of Denmark, DK-2800 Kgs. Lyngby, Denmark*
[2] *NORBLIS IVS, Virumgade 35D, DK-2830 Virum, Denmark*
[3] *DTU Fotonik, Technical University of Denmark, DK-4000 Roskilde, Denmark.*
[4] *Research Center for Non-Destructive Testing (RECENDT), Altenberger Straße 69, 4040 Linz, Austria.*
[5] *NLIR ApS, Hirsemarken 1, 3520 Farum, Denmark.*
[6] *Applied Optics Group, School of Physical Sciences, University of Kent, CT2 7NH Canterbury, United Kingdoms.*
7 *NKT Photonics A/S, Blokken 84, DK-3460 Birkerød, Denmark*

*email: chru@fotonik.dtu.dk

ABSTRACT

We present a mid-infrared spectral-domain optical coherence tomography system operating at 4.1 μm central wavelength with a high axial resolution of 8.6 μm enabled by more than 1 μm bandwidth from 3.58-4.63 μm produced by a mid-infrared supercontinuum laser. The system produces 2D cross-sectional images in real-time enabled the high-brightness of the supercontinuum source in combination with broadband upconversion of the signal to the range 820-865 nm, where a standard 800 nm array spectrometer can be used for fast detection. We discuss the potential applications within nondestructive testing in highly scattering materials and within biomedical imaging for achieving the *in-vivo optical biopsy*.

1. INTRODUCTION

Optical coherence tomography (OCT) has been established as one of the most successful and significant optical techniques for biophotonics and clinical biomedical imaging, most notably within the field of ophthalmology but also within dermatology, oncology, and cardiology. OCT has the ability to perform real-time, non-invasive, and non-contact measurements in reflection, providing 3D sample visualization in a convenient reflection modality. Rapid advances in light sources, detectors, and components for the visible and near-infrared spectral region have enabled the development of advanced functional techniques, high-speed, and high-resolution in vivo imaging, including OCT. In this regard, OCT fills the gap between ultrasonic imaging and confocal microscopy where OCT can offer the non-invasive modality of ultrasound without the need for a contact medium, and high spatial resolution of conventional microscopy without the need for a biopsy. In that sense, OCT is truly an example of the non-invasive optical biopsy. On the other hand, the greatest limitation of OCT is its shallow imaging depth, which is dictated by the scattering of light as it passes through inhomogeneous media. This fundamental property of OCT limits the imaging depth from a few hundred microns to a few millimeters depending on the tissue composition, optical probing scheme, and the wavelength of light. Since scattering losses are inversely proportional to the wavelength of

light relative to the size of the scattering features, it has long been known that the penetration of OCT would benefit from employing a longer center wavelength. Current state-of-the-art commercially available OCT systems for e.g. dermatology operate in the 1.3 μm wavelength range, utilizing the low water absorption, and the maturity of optical fibers and components developed for telecommunications in this region [1]. At longer wavelengths, light sources and detectors are significantly less efficient and components are less matured. In addition, water absorption is generally considered to be too strong for imaging of biological tissue and other aqueous samples in this region, and even in absence of water many materials may have significant vibrational absorption bands in this region. Therefore, the combined effect of absorption and scattering on the penetration depth makes it non-trivial to assess whether a sample would benefit from being imaged at a longer wavelength.

Few attempts have been made to utilize the vast potential of mid-infrared (mid-IR) OCT, such as the early proof of concept work of Colley et al. demonstrating the first in-depth reflectivity profiles in the mid-IR using time-domain OCT. In their work, a single reflectivity profile (A-scan) of a calcium fluoride window and a topographic image of a gold-palladium coated tissue sample were presented. These first measurements were based on quantum cascade laser (QCL) emission and cryogenically cooled mercury cadmium telluride (MCT) detection using a time-domain OCT scheme. With a center wavelength of 7 μm, Colley et al. achieved a 30 μm axial (depth) resolution with an acquisition time of 30 min for a single reflectivity profile, which was heavily affected by side lobes due to the heavily modulated spectral shape. More recently, spectral-domain OCT techniques has been reported in the mid-IR enabled by broadband supercontinuum (SC) lasers, employing either pyroelectric array detection [2] or mid- to- near-IR upconversion detection [3], achieving A-scan rates of 2.5/s and 333.3/s, respectively.

Here, we present results using the mid-IR OCT system reported in [3], as well as initial results using a modified version of the system based on a galvanometer scanning system.

2. THE SYSTEM

The mid-IR OCT system reported in [3] consists of five modular parts: a custom mid-IR SC source based on a 1.55 μm master-oscillator power amplifier (MOPA) pump laser and a single-mode zirconium fluoride fiber, a Michelson interferometer, a translation stage scanning system, an in-house developed frequency upconversion module, and a silicon CMOS-based array spectrometer. Each subsystem is connected via optical fiber to ease the coupling and alignment between subsystems. The mid-IR SC source produces a continuous spectrum from 0.9-4.7 μm and is set to operate at 1 MHz pulse repetition rate generating 40 mW of average power above 3.5 μm. The spectral components below 3.5 μm are blocked by a long-pass filter, resulting in 20 mW coupled to the sample arm of the interferometer. The beam is focused onto the sample using a barium fluoride lens, and images are acquired by moving the sample using motorized translation stages. The sample and reference signals are collected in a single-mode indium fluoride fiber and relayed to the upconversion module for spectral conversion to the near-IR. The upconversion module converts a broad bandwidth from 3576-4625 nm to down to 820-865 nm in a single pass of the crystal. The upconverted signal is then coupled to a multi-mode silica fiber and imaged onto the spectrometer to resolve the spectrum.

The axial/lateral resolution of the system was determined to be approximately 8.6/15 µm from the sensitivity roll-off and by scanning a USAF 1951 resolution test target. Using a translation speed of the fast (horizontal) scanning axis of 3 mm/s, and an integration time of 3 ms per line for maximum signal, 1000 line scans were performed in 3 s resulting in 9 µm horizontal sampling resolution. Along the vertical axis, the resolution was determined by the step size of 10 µm used to move the in the slow scanning axis of the stage. The sensitivity of the system was approximately 60 dB.

In some cases it will not be possible to physically scan the sample, such as in the case of in-vivo optical biopsy. To accommodate this we implemented a galvanometer into the OCT system in order to scan the beam across the sample. A schematic of the modified setup is shown in Figure 1b), and a photograph of the fully packaged, portable 4 µm mid-IR OCT system is shown in Figure 1a).
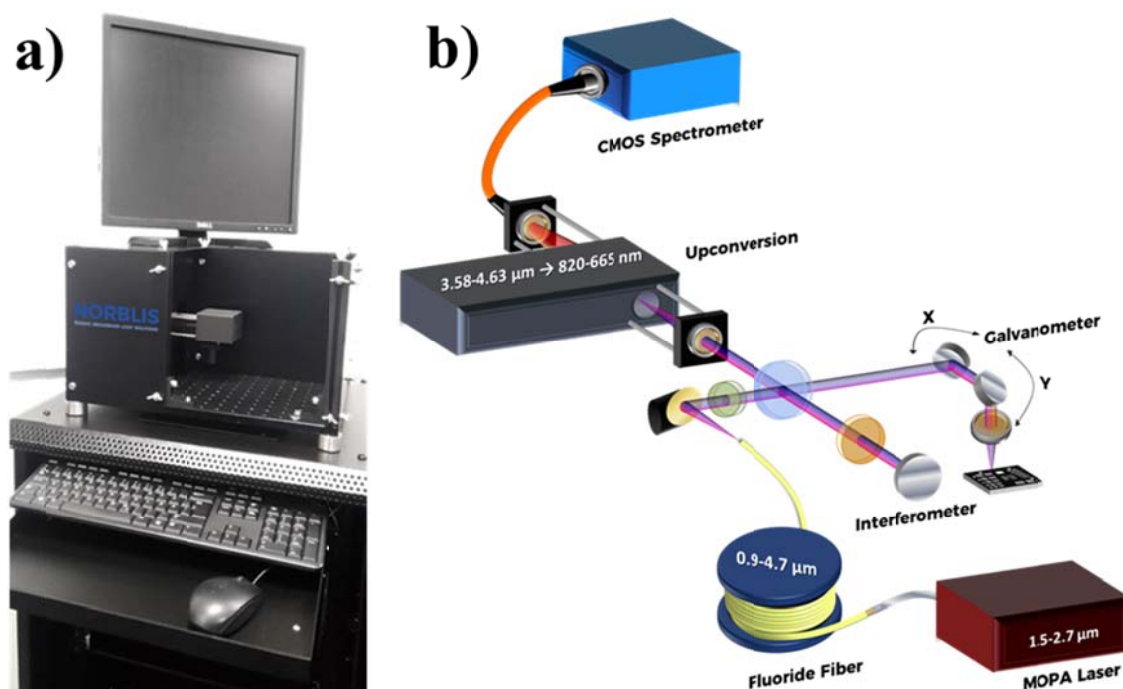

Figure 1. (a) Photograph of the fully-packaged and portable 4 µm OCT system. (b) Schematic setup for the 4 µm OCT system employing a galvanometer scanning system.

3. RESULTS

Ceramics – motorized translation stages

Ceramics are used in wide variety of military, industrial, and medical applications due to their mechanical strength/hardness and chemical resistance. Common uses for ceramics include blades and ballistic protection, brake discs and bearings, and dental and bone implants, respectively. Here we test two common biocompatible ceramics, namely alumina (Al_2O_3) and zirconia (ZrO_2). Figure

2a) shows a photograph of three ceramic plates marked M300 (sintered alumina, 300 μm thickness), CuL (sintered alumina with laser-engraved features, 475 μm thickness), and Z400 (sintered zirconia, 375 μm thickness). It has been previously demonstrated that the penetration depth of 1.7 μm wavelength OCT in alumina is limited to around 300-450 μm, while for zirconia it is approximately 1 mm depending on the surface roughness and porosity [4,5]. Figure 2b) shows the resulting OCT en-face image when stacking the plates with Z400 on top, CuL in the middle (engravings facing downwards), and M300 on the bottom. The OCT system was able to penetrate through first the 375 μm zirconia and then 475 μm alumina to reveal the structures at the bottom. The backside of the M300 plate was not visible; however, the "M" written on the surface with a pencil is clearly seen in the bottom right corner of the image. Figure 2c) shows a similar image obtained when stacking the M300 plate on top and the Z400 plate on the bottom. In this configuration the 4 μm OCT system was able to capture very clear images through both the 300 μm and 475 μm alumina plates, thus demonstrating improved penetration depth compared to previous state-of-the-art. The smoothness of the image in Figure 2c) compared to Figure 2b) is attributed to an increased surface roughness and an increased number of large scattering centers within the zirconia plate.
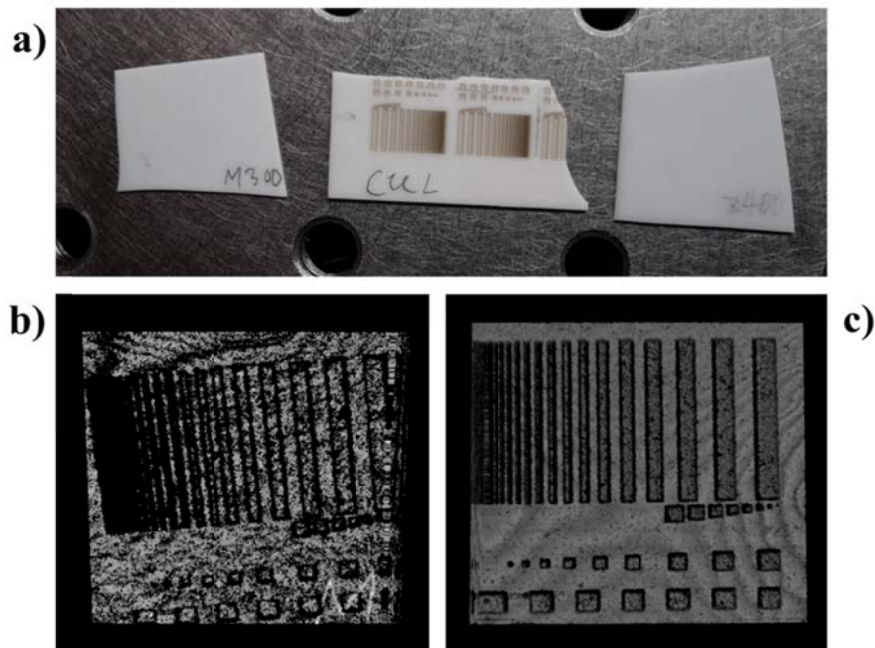

Figure 2. (a) Photograph of the ceramic samples. M300: 300 μm thick alumina, CuL: 475 μm thick alumina with laser-engraved features, and Z400: 375 μm thick zirconia. (b,c) En-face OCT images of laser-engraved features imaged through the Z400+CuL plates, and the M300+CuL plates, respectively.

Artificial skin – galvanometer scanning

To test the galvanometer scanning system for in-vivo optical biopsy an artificial 3D skin model was imaged. The dry skin model was obtained through University Hospital Muenster and has a three-layer structure, as shown in Figure 3a), mimicking real human skin for use in e.g. skin cancer cell

type identification [6]. Figure 3b) shows a C-scan of an artificial skin sample using 1.3 μm OCT, while Figure 3d,f) shows corresponding scans using the 4 μm galvanometer OCT system. It is clear from the 4 μm images that the complex inner structure of the sample is more easily seen at 4 μm due to the reduced scattering. An example of the cross sectionl structure is shown in Figure 3c,e).
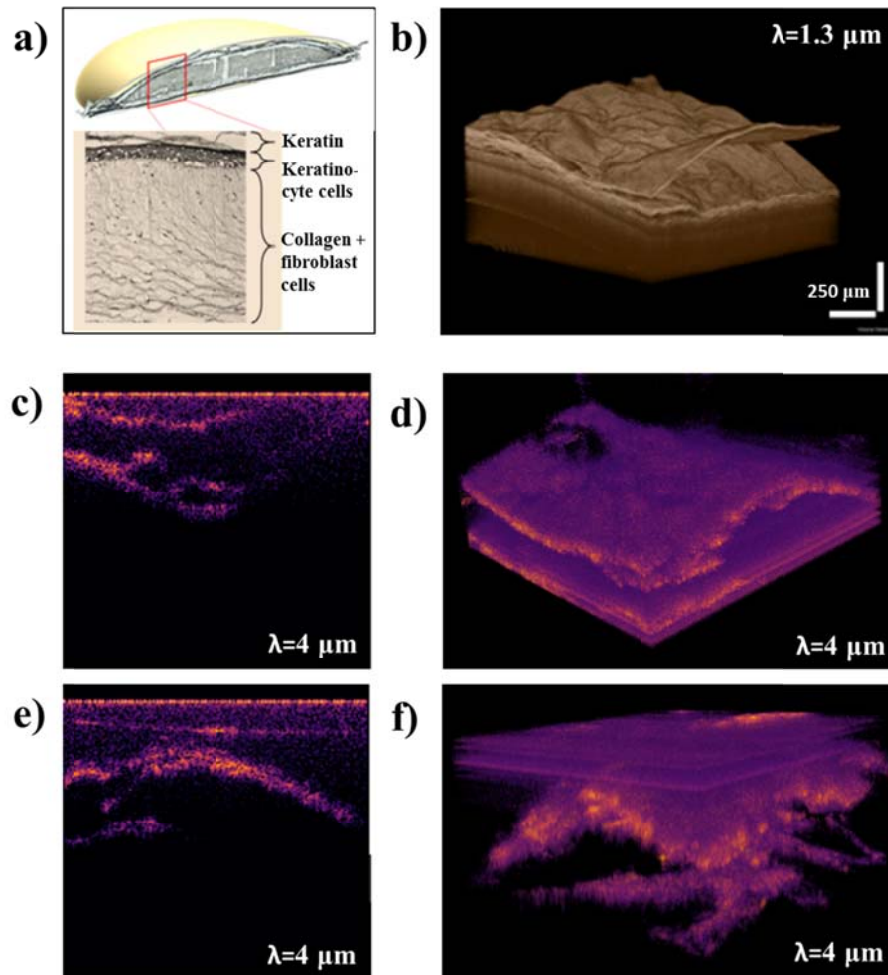

Figure 3. (a) Illustration of the artificial skin model structure. (b) 3D OCT scan of a skin model using 1.3 μm OCT (acquired by NKT Photonics). (c,e) Cross-sectional B-scans of the skin model using 4 μm OCT. (d,f) 3D 4 μm OCT scans of the skin model imaged through the top and bottom, respectively.

A major concern for biomedical imaging is the increased water absorption at long wavelengths, which usually excludes imaging of living biological tissue. However even shallow imaging provides information about structures that are otherwise difficult to assess in a 2D confocal image, and for instance in the case of dermatology the outer layers of the skin consist of dead cells and relatively dry tissue which combined with the fact that skin cancer develops from the surface of the skin means that mid-IR OCT could still be useful for biological imaging. Besides, the spectral region from 3.6-4.6 μm is remarkably devoid of vibrational resonances, making it ideal for imaging using OCT. This principle can also be translated to even longer wavelengths for spectroscopic OCT in the fingerprint

region, which would represent an extension to the recent demonstration of mid-IR raster scanning imaging [7].

4. CONCLUSION

In conclusion, real-time spectral-domain OCT imaging in the mid-IR was demonstrated using a SC source in combination with broadband frequency upconversion covering more than one micron bandwidth from 3.58 to 4.63 μm. The upconverted signal was measured using a Si-CMOS spectrometer acquiring data with a line rate of 0.33 kHz, which enabled real-time B-scans at mm^2/s speed, and 3D-scans at mm^3/min acquisition rate. Furthermore, a galvanometer-based scanning system was implemented and tested for applications within e.g. in-vivo optical biopsy and inspection of bioceramic medical implants.

1. N. M. Israelsen, M. Maria, M. Mogensen, S. Bojesen, M. Jensen, M. Haedersdal, A. Podoleanu, and O. Bang, "The value of ultrahigh resolution OCT in dermatology - delineating the dermo-epidermal junction, capillaries in the dermal papillae and vellus hairs," Biomed. Opt. Express **9**, 2240–2265 (2018).
2. I. Zorin, R. Su, A. Prylepa, J. Kilgus, M. Brandstetter, and B. Heise, "Mid-infrared Fourier-domain optical coherence tomography with a pyroelectric linear array," Opt. Express **26**, 33428–33439 (2018).
3. N. M. Israelsen, C. R. Petersen, A. Barh, D. Jain, M. Jensen, G. Hannesschläger, P. Tidemand-Lichtenberg, C. Pedersen, A. Podoleanu, and O. Bang, "Real-time high-resolution mid-infrared optical coherence tomography," Light Sci. Appl. **8**, 11 (2019).
4. R. Su, M. Kirillin, E. W. Chang, E. Sergeeva, S. H. Yun, and L. Mattsson, "Perspectives of mid-infrared optical coherence tomography for inspection and micrometrology of industrial ceramics," Opt. Express **22**, 15804–15819 (2014).
5. R. Su, E. Chang, P. Ekberg, and L. Mattsson, "Enhancement of probing depth and measurement accuracy of optical coherence tomography for metrology of multi-layered ceramics," in *1st International Symposium on Optical Coherence Tomography for Non-Destructive Testing,* (n.d.), pp. 71-73 (2013).
6. L. Kastl, B. Kemper, G. R. Lloyd, J. Nallala, N. Stone, V. Naranjo, F. Penaranda, and J. Schnekenburger, "Mid-infrared spectroscopy in skin cancer cell type identification," in A. Amelink and I. A. Vitkin, eds. (2017), p. 104130S.
7. C. R. Petersen, N. Prtljaga, M. Farries, J. Ward, B. Napier, G. R. Lloyd, J. Nallala, N. Stone, and O. Bang, "Mid-infrared multispectral tissue imaging using a chalcogenide fiber supercontinuum source," Opt. Lett. **43**, 999–1002 (2018).